Title

UV-Induced Reaction Pathways in Bromoform Probed with Ultrafast Electron Diffraction

Journal

Journal of the American Chemical Society, 146(41)

ISSN

0002-7863

Authors

Hoffmann, Lars

Toulson, Benjamin W

Yang, Jie

et al.

Publication Date

2024-10-07

DOI

10.1021/jacs.4c07165

Peer reviewed

UV-induced reaction pathways in bromoform probed with ultrafast electron diffraction

Lars Hoffmann,[1,2] Benjamin W. Toulson,[1] Jie Yang,[3†] Catherine A. Saladrigas,[1,2] Alfred Zong,[2,4] Sri Bhavya Muvva,[5] Joao Pedro Figueira Nunes,[5§] Alexander Reid,[3] Andrew R. Attar,[3] Duan Luo,[3ξ] Fuhao Ji,[3] Ming-Fu Lin,[3] Qingyuan Fan,[3] Stephen Weathersby,[3] Xiaozhe Shen,[3] Xijie Wang,[3η] Thomas J. A. Wolf,[3] Daniel M. Neumark,[1,2] Stephen R. Leone,[1,2,6] Michael W. Zuerch,[2,4] Martin Centurion[5] and Oliver Gessner[1]*

[1]Chemical Sciences Division, Lawrence Berkeley National Laboratory, Berkeley, California 94720, USA

[2]Department of Chemistry, University of California, Berkeley, California, 94720, USA

[3]SLAC National Accelerator Laboratory, Menlo Park, California 94025, USA

[4]Materials Sciences Division, Lawrence Berkeley National Laboratory, Berkeley, California 94720, USA

[5]Department of Physics and Astronomy, University of Nebraska–Lincoln, Lincoln, Nebraska 68588, USA

[6]Department of Physics, University of California, Berkeley, CA 94720, USA

ABSTRACT: For many chemical reactions it remains notoriously difficult to predict and experimentally determine the rates and branching ratios between different reaction channels. This is particularly the case for reactions involving short-lived intermediates, whose observation requires ultrafast methods. The UV photochemistry of bromoform ($CHBr_3$) is among the most intensely studied photoreactions. Yet, a detailed understanding of the chemical pathways leading to the production of atomic Br and molecular Br_2 fragments has proven challenging. In particular, the role of isomerization and/or roaming and their competition with direct C-Br bond scission has been a matter of continued debate. Here, gas-phase ultrafast megaelectronvolt electron diffraction (MeV-UED) is used to directly study structural dynamics in bromoform after single 267 nm photon excitation with femtosecond temporal resolution. The results show unambiguously that isomerization contributes significantly to the early stages of the UV photochemistry of bromoform. In addition to direct C-Br bond breaking within <200 fs, formation of iso-$CHBr_3$ (Br-CH-Br-Br) is observed on the same timescale and with an isomer lifetime of >1.1 ps. The branching ratio between direct dissociation and isomerization is determined to be 0.4±0.2:0.6±0.2, i.e., approximately 60% of molecules undergo isomerization within the first few hundred femtoseconds after UV excitation. The structure and time of formation of iso-$CHBr_3$ compare favorably with the results of an ab initio molecular dynamics simulation. The lifetime and interatomic distances of the isomer are consistent with the involvement of a roaming reaction mechanism.

Introduction

The photochemistry of halogenated hydrocarbons is of significant importance due to their atmospheric ozone damaging capability.[1] Bromoform ($CHBr_3$) is the primary precursor for atomic bromine in the troposphere as well as the stratosphere, where it is particularly impactful due to the high efficiency of catalytic ozone destruction.[2] Even though the concentration of Br in the atmosphere is lower than that of Cl, atomic bromine is ~40-100 times more efficient in depleting ozone on a per atom basis.[3,4] Despite numerous studies that span more than three decades,[5–11] disentangling the UV photochemistry of bromoform ($CHBr_3$) has proven extraordinarily challenging. Experimental and theoretical yields for the UV induced elimination of Br_2 molecules, for example, vary by orders of magnitude and ultrafast spectroscopy experiments have not converged on a canonical picture for the reaction pathways that dominate the earliest UV relaxation dynamics within the first few picoseconds after photoexcitation.

Multiple reaction intermediates and products are energetically accessible by one-photon 267 nm (4.64 eV, 448 kJ/mol) excitation:

$CHBr_3 + h\nu \rightarrow CHBr_2 + Br$	267 kJ/mol[9]	(I)
$CHBr_3 + h\nu \rightarrow CHBr + Br_2$	349 kJ/mol[9]	(II)
$CHBr_3 + h\nu \rightarrow CBr_2 + HBr$	247 kJ/mol[9]	(III)
$CHBr_3 + h\nu \rightarrow CBr_3 + H$	402 kJ/mol[12]	(IV)
$CHBr_3 + h\nu \rightarrow$ iso-$CHBr_3$	209 kJ/mol.[13]	(V)

Energy values are stated relative to the $CHBr_3$ ground state. Channel V refers to the formation of a Br-CH-Br-Br isomer, where one of the parent molecule C-Br bonds is removed and a C-Br-Br bond linkage is formed. Channel (I) has previously been determined to be the dominant reaction pathway at 267 nm, with a measured quantum yield of 0.76±0.03.[7] The importance of Br_2 as a dissociation product has been a matter of debate. For 267 nm excitation, quantum yields of up to 0.16 have been reported.[8] However, it has also been proposed that a considerable, potentially

dominating fraction of Br_2 production in several experiments has been due to multiphoton absorption via sequential excitation of $CHBr_3$ and an intermediate $CHBr_2$ radical.[9,14,15] No significant contributions from HBr and H products (Channels III and IV) after single photon excitation around 267 nm have been reported.

The barrier for isomerization (Channel V) has been located slightly below the threshold for direct dissociation to form Br radicals (Channel I), implying an important role of isomerization in bromoform photochemistry.[13,16,17] For sufficiently high excitation energies, the iso-$CHBr_3$ configuration is expected to be an important intermediate towards both atomic Br elimination through Br-Br bond scission and Br_2 production by cleaving off the Br-Br fragment.[13,16–18] For excitation with 267 nm radiation of isolated $CHBr_3$ molecules, microcanonical transition-state (RRKM) calculations predict that the majority of molecules (≈ 70%) will initially undergo isomerization (Channel V), with the remaining fraction undergoing direct dissociation to form atomic Br (Channel I).[13] These calculations also predict that iso-$CHBr_3$, once formed, will predominantly dissociate into $CHBr_2$ + Br, with the alternative CHBr + Br_2 dissociation contributing only ∼2%, corresponding to an overall molecular Br_2 yield of ≲ 1.4%. The latter number takes into account the isomerization yield and the fact that the internal conversion yield after UV excitation is less than unity.[13] Until now, no experimental determination of the branching ratio for the formation of the parent molecular isomer after UV excitation of bromoform has been achieved.

Most experimental studies of iso-$CHBr_3$ have been conducted on bromoform in solution, usually in organic solvents such as cyclohexane or acetonitrile.[10,19,20] The solvent environment enables formation of iso-$CHBr_3$ through a recombination mechanism that is not available in the gas phase. In this mechanism, the radical fragments after C-Br bond cleavage are confined by the solvent cage, eventually leading to recombination to the isomer. The solvent also dissipates excess energy to further stabilize and increase the lifetime of iso-$CHBr_3$, which can be on the order of picoseconds to microseconds and is strongly dependent on the solvent.[19] However, an alternative mechanism has also been proposed, in which ultrafast concerted excited-state isomerization occurs through a conical intersection between the lowest-lying singlet state of $CHBr_3$ and the ground-state of iso-$CHBr_3$.[20] This suggestion is based on the observation of a sub-100 fs formation channel of iso-$CHBr_3$, which is too fast for recombination mediated by the solvent cage. UV-vis transient absorption spectroscopy of gas-phase bromoform using 250 nm excitation provided support for this hypothesis, where a short-lived feature assigned to iso-$CHBr_3$ has been observed with rise and decay times of 50 fs and 85 fs, respectively.[11,21] A combined femtosecond transient XUV absorption and ab initio molecular dynamics (MD) study on 268 nm excited $CHBr_3$ observed very similar timescales but assigned a rather minor role of the isoform intermediate. Instead, the two characteristic timescales for spectral changes were mainly associated with a very fast (∼40 fs) initial symmetry change of the molecule due to the C-Br recoil action, followed by a slower (≳ 85 fs) elimination of a Br fragment.[22]

Evidently, the relative importance of the isomerization pathway after UV excitation of isolated bromoform molecules is still a matter of debate and requires further investigation. Here, we probe the temporal evolution of the nuclear geometries of $CHBr_3$ following 267 nm excitation by gas phase ultrafast electron diffraction (UED). Femtosecond dynamics of the atomic rearrangements are reconstructed in real-space from the momentum space UED traces, giving direct insight into the isomerization and dissociation trajectories of bromoform with sub-Ångstrom spatial resolution and ∼150 fs temporal resolution.[23] Both momentum space and real-space analyses of the UED data indicate a competition between direct dissociation into $CHBr_2$+Br and the formation of iso-$CHBr_3$ in the gas-phase. In contrast to previous findings that indicated a sub-100 fs lifetime of the isoform after 250 nm excitation,[11,21] the UED measurements suggest that iso-$CHBr_3$ configurations are present for more than 1 ps after 267 nm excitation. In fact, Br-CH-Br-Br formation is found to account for (60±20)% of the initial UV photoreaction yield, while (40±20)% of molecules undergo direct dissociation to form atomic Br on sub-ps timescales. The relative yields are close to those predicted by the RRKM calculations of Kalume et al. (70% isomerization vs. 30% direct dissociation at 267 nm excitation[13]) for dynamics on the electronic ground state. The observed rates of formation, however, differ by approximately an order of magnitude from the results of these calculations, which predict isomerization within 4.2 ps, direct Br atom elimination within 10 ps, and Br atom elimination after isomerization within 370 fs. The observed isomerization within ≤ 200 fs and the structure of the isomer are reproduced by excited state ab initio MD simulations. The UED data indicate that both isomerization and direct dissociation proceed along very similar molecular geometries up to ∼200 fs after UV excitation, when the two reaction pathways separate and either result in the formation of the Br-CH-Br-Br isomer or the ejection of a bromine atom (Br-CH-Br + Br). Two pictures are discussed to rationalize the findings. In the first, the molecular wavepacket reaches a saddle point of the multidimensional potential energy surface (PES) after ∼200 fs and small changes in the approach and the PES topography may lead to significantly different outcomes of the reaction. The second picture employs a roaming mechanism, similar to the one proposed by Tarnovsky and coworkers,[11,21] but with the key distinction that dissociation of the isoform appears to be much slower than previously suggested, which could open a pathway for production of Br_2 fragments on timescales >1 ps.

Experiment

The experiment utilizes the relativistic mega-electronvolt (MeV) UED facility at SLAC National Accelerator Laboratory.[24–27] A schematic of the experimental setup is shown in Fig. 1. The sample (Bromoform, 99%) is commercially purchased and used without further purification. Bromoform vapor is injected into a gas flow cell in the reaction chamber with a vapor pressure of 670 Pa at 20 °C. A linearly polarized pump laser with a central wavelength of 267 nm

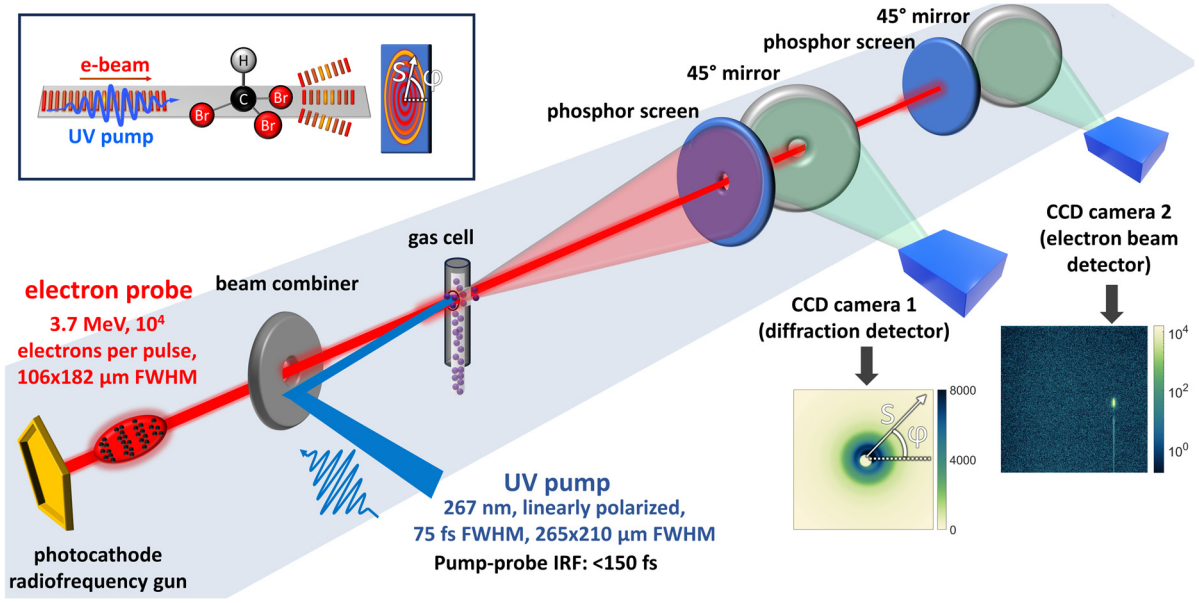

Figure 1. Schematic of the experimental setup. UV pump and electron probe coincide on the gas sample. The diffraction pattern is collected on the first CCD camera while the undiffracted beam is detected at the second CCD camera. Inset: sketch of the scattering process.

is focused in front of the 600 µm diameter entrance hole of the gas cell. The laser and the electron beam are operated at a 360 Hz pulse repetition rate. The laser pulse duration is estimated to 75 fs and the nominal spot size to 265 µm × 210 µm (horizontal × vertical, full-width-at-half-maximum, FWHM). The UED data indicates an excitation ratio of 0.5%, which corresponds to a pump fluence of approximately 10 mJ/cm^2. By using a 45° drilled-through mirror, the pump beam is spatially overlapped with the electron beam in close to parallel alignment (~3°). The electron beam has a kinetic energy of 3.7 MeV and is focused to a 106 µm × 182 µm (horizontal × vertical, FWHM) spot. The temporal width of the instrument response function is determined to be ≤ 150 fs (FWHM), using ultrafast heating of bismuth (see Supporting Information (SI)).[28] Diffraction images are recorded by a combination of a phosphor screen (P43) with a center hole, a 45° mirror with a center hole, and an electron multiplying charged-coupled device (EMCCD) camera. Each image is integrated for 10 s before read-out. The main undiffracted electron beam passes through the hole in the first mirror and is then imaged by a second phosphor screen/mirror/CCD camera setup, which also includes a bending magnet (not shown) for electron energy spread measurements. As detailed in the SI, significant efforts are made to ensure that multiphoton excitation processes do not notably contribute to the observed dynamics.

Results

Figure 2 shows a) the modified scattering intensity sM(s) and b) the atom pair distribution function PDF(r) for ground state bromoform. Red curves are measured, blue curves simulated using the independent atom model (IAM). A detailed description of the IAM and the data analysis is provided in the SI. The two most prominent features in the PDF correspond to the C-Br and Br-Br distances in bromoform, centered at 1.93 Å and 3.22 Å, respectively. The positions and amplitudes exhibit excellent agreement with the simulated data that are based on the tabulated structure of bromoform in the NIST database.[29] Signals related to the hydrogen atom are of much smaller amplitude as the scattering intensity scales with the atomic number Z. We exclude the hydrogen atom from further analysis and discussion because its contribution to the overall scattering intensity is too small to be discerned.

Figures 3a and 3b show false-color maps of the time-dependent ΔI/I(Δt) and ΔPDF(Δt) signals, respectively, for pump-probe delays Δt between –0.6 and 1.1 ps. Here, ΔI refers to scattering signal intensity differences induced by the 267 nm excitation and ΔPDF to corresponding changes in the PDF. To reduce noise, both maps are convoluted along the time axis with a 150 fs FWHM Gaussian function.

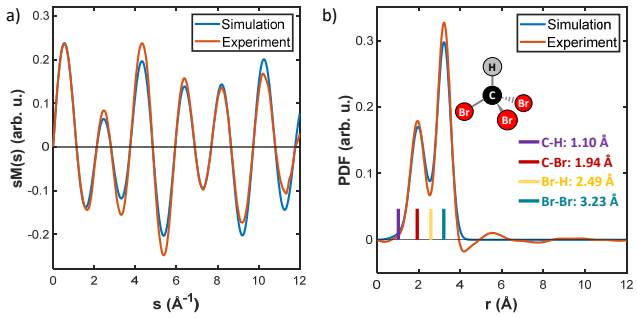

Figure 2. Static diffraction of bromoform. a) Modified scattering intensity sM(s) in momentum space. b) Pair distribution function (PDF) of ground-state bromoform in real space obtained by Fourier sine transformation of a). The color bars indicate NIST tabulated atom pair distances. Red curves are from the experiment, blue curves from a simulation using the independent atom scattering model.

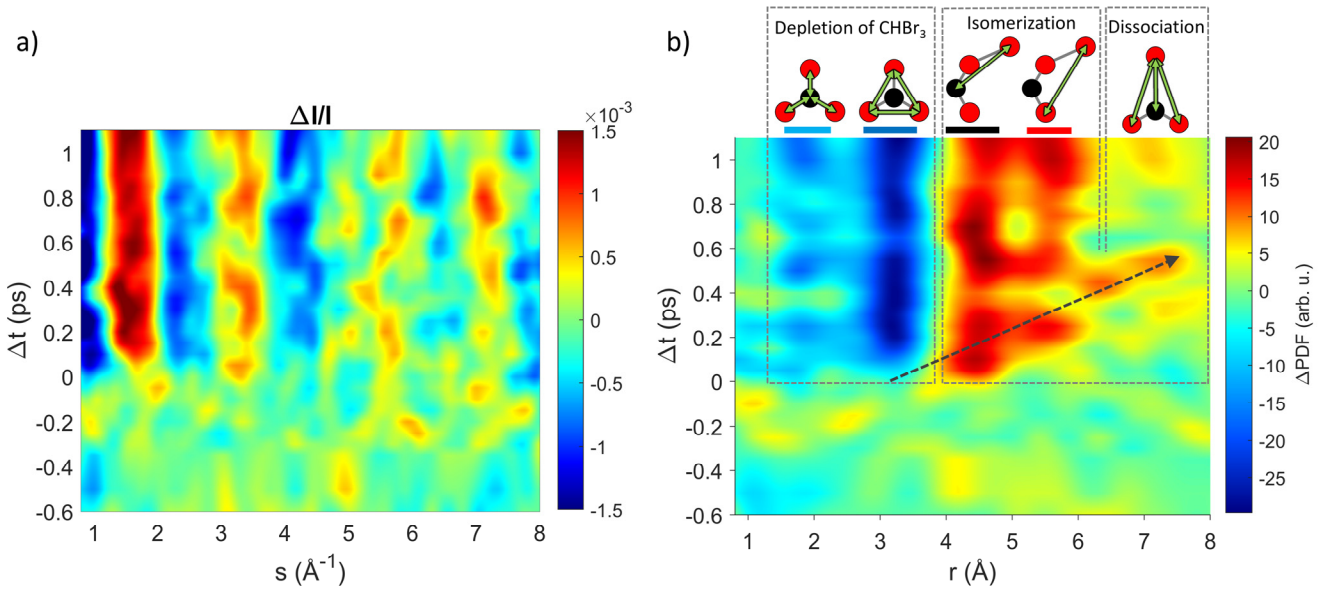

Figure 3. Time-dependent scattering results. a) The relative diffraction difference ΔI/I shows the time-dependent change of scattering intensities in momentum space. b) The experimental ΔPDF indicates two different product channels (red signals): isomerization (vertical features) and dissociation (diagonal feature).

Multiple features are readily apparent in Fig. 3b. At short interatomic distances r < 4 Å, two dominant negative (blue) signals indicate the depletion of parent molecule C-Br (1.9 Å) and Br-Br (3.2 Å) bond lengths, corresponding to the loss of ground state population. For values r ≳ 4 Å, a series of positive (red) signals reveals the appearance of multiple new interatomic distances after photoexcitation. Two types of photoinduced configurations can be distinguished: one with constant distances across the 1.1 ps range of positive pump-probe delays (vertical red lines) and another one with a fast-increasing interatomic distance, leading to the diagonal positive (red) signal marked with a dashed arrow. The two vertical red features are centered at approximately 4.5 Å and 5.6 Å. These values are within the range of theoretical estimates of the C-Br_{iso} and Br-Br_{iso} bond lengths in the relaxed Br-CH-Br-Br isomer configuration, which vary between ~3.8–4.5 Å and ~4.8–5.8 Å, respectively.[11,13,16,18,22] Accordingly, we associate the vertical positive signals with the emergence of the Br-CH-Br-Br isomer as indicated in Fig. 3b. The average slope of the signal associated with an increasing interatomic distance is ~8±2 Å/ps. Given the uncertainty of the slope reading, this value is in reasonable agreement with the result of a recent MD simulation, which estimates that the average Br-Br distance during direct, 268 nm pump-induced dissociation increases by ~10 Å/ps.[22] Thus, we associate the diagonal signal with direct dissociation of bromoform and the ultrafast release of a Br radical.

Analysis & Discussion

The real-space representation in Fig. 3b provides an intuitive assessment of the photoinduced structural changes in the molecule. Yet, the finite detector range, in particular around the central hole (Fig. 1), can lead to artifacts during the sine transformation. In contrast, the momentum-space representation provides a more pristine portrayal of the data that is better suited for quantitative analysis of the different reaction pathways. Consequently, all quantitative statements in this work are derived from fit procedures applied to momentum space data as described in the following. We develop a description of the measured ΔI(s,Δt) distributions in momentum space based on a model that includes two pathways: isomerization (Channel V) and direct dissociation (Channel I). To avoid too many degrees of freedom in the fit and hence ill-defined fit results, the dissociation channel is restricted to symmetric configurations with the departing Br atom propagating along its original C-Br bond axis, while the remaining molecular backbone is kept frozen. In contrast, no symmetry restriction is applied to the isomerization channel and interatomic distances can vary across a wide range of values. Details of the model and fit procedure are provided in the SI. After performing the momentum-space fit of the UED data, self-consistency of the resulting time-dependent molecular configurations and branching ratios is verified by comparing the real space transform of the fit results with the experimental ΔPDF(Δt) map.

The global fit results in momentum space are shown in Fig. 4a. Figure 4b shows the real space transform of the fit results and Fig. 4c an average of 113 trajectories from MD simulations, which exhibits a similar slope of the dissociative Br signal. The fit extends across a momentum range of 0.8 Å – 6 Å. ΔPDF is convoluted with a 150 fs (FWHM) wide Gaussian along the time delay axis to reduce the impact of noise. The map in Fig. 4b matches the experimental ΔPDF in Fig. 3b well, confirming self-consistency of the two-channel relaxation model and the momentum space analysis. A more detailed discussion in the SI also shows that the key features of the experimental ΔPDF are qualitatively unaffected by the limited momentum range of the measurements. Even though the global fit uses a simplified model, it provides a good match to the experimental data.

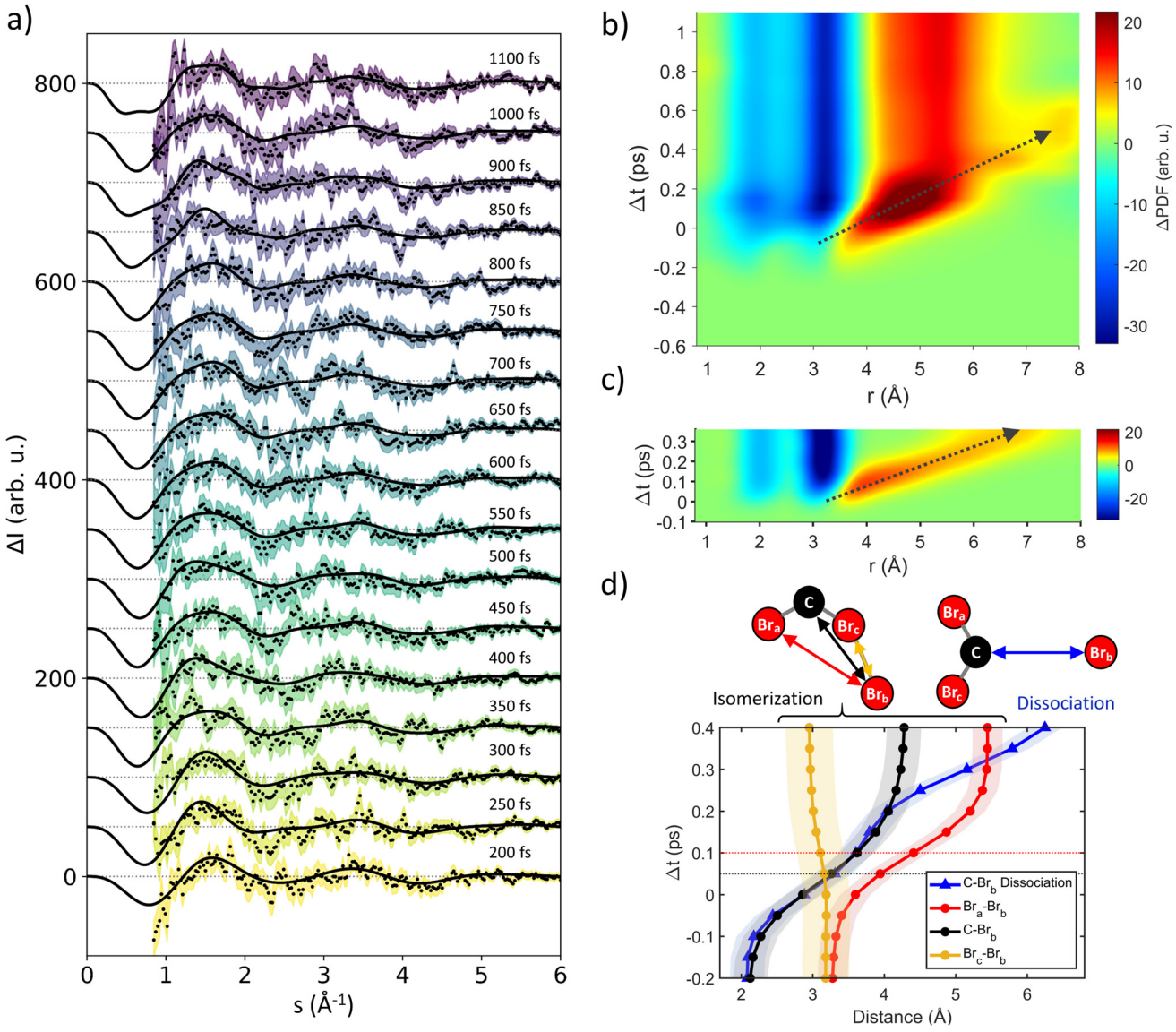

Figure 4. Trajectories obtained by fitting experimental ΔI in momentum space. a) Time-dependent momentum space difference signals ΔI (circles) and fit results (solid lines) for Δt=200 fs – 1100 fs. For better clarity, the traces are offset vertically. Shaded areas represent twice the standard error of the mean. b) ΔPDF obtained from the fit. c) Simulated ΔPDF from an average of 113 MD simulation trajectories. d) Key structural dynamics in the range Δt=-200 fs – 400 fs. Filled circles and solid lines indicate the fit results. The black and red horizontal dotted lines indicate the half points of the rising edges of the average C-Br_b and Br_a-Br_b distances, respectively. Their vertical offset corresponds to an expected delay due to the larger mass of the Br atoms compared to the C atom.

In addition to the smooth isomerization trajectory trends seen in Fig. 4b,d, we have also considered the possibility that the time-dependent intensity modulations noticeable in Fig. 3b in the range of the isomer may be connected to vibrational dynamics. However, the apparent intensity modulation period of ~500 fs does not map well onto any of the calculated vibrational modes of iso-$CHBr_3$.[11,13] While we cannot exclude that the modulations are related to the superposition of several vibrational modes, we refrain from reading such a level of detail into the currently available data.

Note that the two-channel global fit model described above is applicable only for the range Δt = 200–1100 fs, where the isomer and dissociative molecule signals are separable (see Figs. 3b, 4b). Data for shorter delays are fitted separately, using a two-structure approach where both geometries can vary freely, but the branching ratio between the two channels is fixed to the ratio derived in the global long-delay range fit. Figure 4d shows the key atomic pair distances of the dissociation and isomerization trajectory for early delays between -200 fs and 400 fs. See SI for details and a comparison of the experimental trajectories to the results of the MD simulations.

Interestingly, the C-Br distances of the direct dissociation and the isomerization pathways evolve identically up to ~200 fs after UV excitation. From this point onward, the two curves separate rapidly, whereby the dissociative motion appears to accelerate, while the isomerization curves

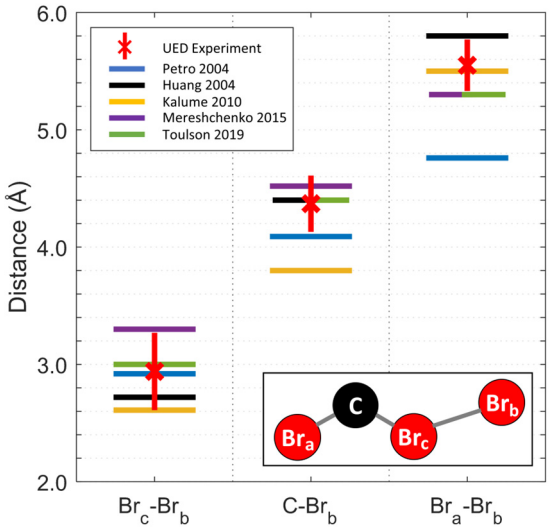

Figure 5. Experimentally determined iso-$CHBr_3$ structure (red crosses and error bars) compared to theoretical predictions (horizontal bars). The corresponding references are Petro 2004,[18] Huang 2004,[16] Kalume 2010,[13] Mereshchenko 2015,[11] and Toulson 2019.[22]

flatten out, indicating that iso-$CHBr_3$ has been formed and is stable on the timescale of the measurement. In contrast, in the MD calculations, the trajectories passing by the isomer geometry continue toward dissociation more quickly (see SI). For delays < 200 fs, the increase in C-Br distance notably precedes the corresponding increase in Br-Br distances for both the UED measurement (horizontal dotted lines) as well as the MD simulations. This effect is due to the relatively light carbon atom accelerating faster than the three heavy bromine atoms during the first tens of femtoseconds after excitation. The fact that the UED results reproduce this subtle detail of the intramolecular dynamics lends additional credence to the technique and the analysis performed herein.

Figure 5 shows a comparison of the experimentally determined isomer structure (red crosses with vertical error bars) with various theoretical predictions (horizontal bars).[11,13,16,18,22] The theoretical estimates straddle the experimental values of 2.9 Å, 4.4 Å and 5.6 Å for the Br_b-Br_c, C-Br_b and Br_a-Br_b interatomic distances, respectively, with most theoretical values contained within the experimental uncertainty. Overall, best agreement is achieved between the experiment and the minimum energy iso-$CHBr_3$ configuration calculated by Toulson et al. for the T_1 surface, which is considered the primary excited state at 267 nm.[22] We note, however, that most of the reported isomer configurations for both ground (S_0)[11,13,16-18] and excited (T_1)[22] electronic states are compatible with the experimental results reported here within their uncertainties. Thus, the electronic character of the observed isoform remains to be determined.

The UED results shown in Fig. 5 provide the first experimental characterization consistent with the long-predicted Br-CH-Br-Br isomer configuration that is accessed after UV excitation of bromoform. In contrast to the findings of our previous work, using femtosecond XUV transient absorption measurements in combination with ab-initio MD simulations,[22] the UED measurements presented here indicate that the isomer configuration plays a substantial role for the 267 nm pump-induced UV photochemistry of bromoform. From the momentum fit results presented in Fig. 4a, the branching ratio between the two reaction channels is determined to be 0.4 ± 0.2 for the direct dissociation and 0.6 ± 0.2 for the isomer channel. The uncertainties are estimated by the method described by Cumpson and Seah.[30] Details are provided in the SI. The measurements show that the reaction pathways for the majority of photoexcited molecules proceed through the isomer geometry. This observation agrees with the results of RRKM calculations by Kalume et al. for hot electronic ground state molecules,[13] which predict that approximately 70% of bromoform molecules would undergo isomerization after 267 nm excitation, while the remaining 30% would directly dissociate to release a Br atom. This ratio lies within the uncertainty range of the experimental values presented here. The lifetime of the isomer, however, indicated by the UED results, is significantly longer than previously reported. Based on a series of gas phase ultrafast visible transient absorption spectroscopy measurements, Tarnovsky and co-workers concluded that the isomer is formed on a sub-100 fs timescale and dissociates within less than 200 fs after photoexcitation with 250 nm.[11,21] In the measurements presented here, the isomer forms within 200 fs and is stable for at least 1.1 ps after the 267 nm excitation. While the difference in excitation energies could potentially play a role for the discrepancy, it is interesting to note that the overall timescale for the appearance and decay of the isomer reported previously is very similar to the timescale observed here during which both the directly dissociating population of molecules and the molecules that reach the isomer pass through a region of very similar geometries (Fig. 4d). Thus, to a certain degree, it may become a matter of semantics for the earliest dynamics whether a particular intermediate configuration may be termed a very short-lived isomer or a dissociating molecule. Yet, the longer-lived isomer population observed here has clearly been missed by previous experiments. The trajectories of the photoexcited bromoform molecules will sample a large range of geometries and the distinction between isomerization and direct dissociation will not always be clear-cut. However, the results shown in Fig. 4 clearly demonstrate that a distinct separation of pathways is taking place approximately 200 fs after photoexcitation, whereby ~40 % of molecules expel a Br radical, while ~60 % of the excited population form a Br-CH-Br-Br isomer with a lifetime beyond 1.1 ps.

For bromoform in solution, isomer lifetimes from picoseconds to nanoseconds have been reported.[10,19] But unlike the solvent case, iso-$CHBr_3$ in the gas phase is unable to be stabilized by energy transfer to its surroundings. The experimentally observed >1.1 ps gas phase isomer lifetime is longer than the 370 fs isomer dissociation timescale predicted by Reid and co-workers (for 267 nm excitation) based on ground state RRKM calculations.[13] The ~200 fs

appearance time of the isomer in the UED experiment deviates even further from the RRKM results, which predict isomerization within 4.2 ps. Considering that, as noted above, the RRKM determined branching ratio between isomerization and direct dissociation agrees quite well with the experiment, it is surprising that the absolute rates for the different reaction channels differ significantly from the measurements. The dominant Br radical production channel in the calculations is through isomerization within 4.2 ps, followed by dissociation within 370 fs, which would lead to a Br signal in the experiment with a slowly (multiple ps) rising edge that is delayed by a few hundred fs compared to zero pump-probe delay. In contrast, the experimental signal appears within ~200 fs and remains constant within the experimental resolution. As shown in Fig. S11, the earliest dynamics and the rate of formation of the isomer agrees reasonably well with the results of a previous MD simulation launched on the T_1 electronic surface.[22] The same calculation, however, severely underestimates the relative yield and stability of the isoform.

A possible explanation for these observations is that the molecular wavepackets encounter a saddle point of the multi-dimensional potential energy surface (PES) approximately 200 fs after UV excitation. In this picture, slight variations in the approach of the saddle point by the wavepackets may lead to distinctly different outcomes. Encountering a steep slope along the C-Br coordinate in the vicinity of the saddle point leads to accelerated dissociation, while isomerization takes place within the flatter region of the PES. Predicting the precise PES structure and, consequently, the dynamics in the vicinity of such saddle points are notoriously challenging.[31-33] Very small variations can lead to significantly different outcomes, which may explain the discrepancy between the ~2% isomerization yield predicted by the MD simulations[22] and the ~60% yield determined here.

Another, related mechanism to consider is a roaming reaction. Here, a radical does not completely separate from a molecule, but enters an extended trajectory in its vicinity, which can lead to reattachment and/or intramolecular abstraction.[34-37] Indeed, a roaming type reaction was previously reported for 250 nm excited $CHBr_3$, in which one of the Br atoms migrates towards another Br atom to transiently form a geometry reminiscent of iso-$CHBr_3$.[11] Albeit, the calculated trajectory followed that of a direct dissociation and did not approach the optimized iso-$CHBr_3$ structure. The formation and decay of the transient structure, primarily by Br radical abstraction, was indicated to be complete within ~200 fs.[11,21] In contrast, the isoform observed here matches the theoretically predicted structure, forms within 200 fs and persists for at least 1.1 ps. Several aspects of the UED results are consistent with the involvement of a roaming-type mechanism.

The definition of roaming reactions has evolved over time as more knowledge is gained regarding their various forms of manifestation.[34,38-41] One recently proposed definition refers to a roaming reaction as "one that yields products via reorientational motion in the long-range (3–8 Å) region of the potential" and, more generally, refers to this range as the van der Waals region.[34,37,40] The ultrafast isomerization of bromoform as seen in Fig. 4 and 5 involves the formation of a metastable Br_c-Br_b bond with a ~3 Å atom-atom spacing. While the boundaries of the above roaming definition are somewhat soft and may depend to a certain degree on the size of the participating atoms, the dynamics and intramolecular distances observed here appear to fall within the range of possible roaming trajectory candidates.[42]

The large discrepancy of the observed rates of formation and decay to RRKM calculations may also indicate that isomerization does not proceed through a transition state but could involve roaming trajectories that are not captured by RRKM rates. Moreover, a common characteristic of roaming type reactions is that they proceed in flat regions of the PES landscape, typically associated with low frequencies and relatively long timescales, up to nanoseconds.[34,41,43] This aspect of roaming is consistent with the observed >1.1 ps lifetime of iso-$CHBr_3$. We note, however, that none of the described observations provide definitive evidence for the involvement of a roaming-like reaction pathway. Clearly, more theoretical work is needed to further elucidate the mechanism underlying the observed dynamics, which is beyond the scope of this work.

An important aspect of this much needed work is the determination of the electronic character of the observed isoform. UV excitation from the S_0 ground state with 267 nm corresponds to an n(Br) → σ*(C–Br) transition, i.e., the promotion of an electron from a nonbonding Br orbital to a σ* orbital along the C-Br bond.[6,20] For excitation wavelengths >240 nm, it has been proposed that contributions from either the triplet[6] or the singlet[20] manifold of low-lying electronic states dominate the initially excited configuration. Based on the calculated energies and oscillator strengths for transitions from S_0 in the region ~240 nm - 270 nm,[6] which are entirely dominated by the triplet manifold, we conclude that the 267 nm excitation in the current experiment predominantly populates the lowest lying triplet state, $\tilde{a}^3A_2$ ("T_1"), possibly with some contributions from the slightly higher lying $\tilde{b}^3E$ ("T_2") and $\tilde{c}^3A_1$ ("T_3") states. Accordingly, the MD simulations in ref. [22] were initiated on the T_1 surface. See additional details in the SI. The calculations do not include spin-orbit coupling, which limits the range of accessible potential energy surfaces to the triplet manifold. Previous studies, however, concentrated on calculating isobromoform configurations in the S_0 singlet electronic ground state,[11,13,16-18] often in the context of modeling the emergence of molecular fragments after UV excitation (see below). Tarnovsky and co-workers proposed that, upon 250 nm excitation, the molecular wavepacket is launched on the S_1 state and relaxes back to a hot S_0 configuration within less than ~40 fs due to efficient S_1/S_0 coupling via a conical intersection.[11,21] In this picture, a ground state isoform is present almost immediately after passage through the CI and has a lifetime of less than 150 fs, leading to dissociation into $CHBr_2$ + Br within less than ~200 fs after photoexcitation. Given the extremely short timescales involved and the rather symmetric trajectories predicted in these studies, they would be indistinguishable from the direct dissociation path in the current UED study. Thus, a different

mechanism must be at play to explain the much more slowly (~200 fs) appearing and much longer (> 1.1 ps) lived isoform configurations observed here. Given all available information, we speculate that an MD simulation similar to that in ref. [22] but extended to include spin-orbit coupling and allowing for relaxation to the S_0 ground state surface may provide a path toward a better understanding of the configurations and dynamics reported herein. Additionally, the inclusion of excitations to the higher lying triplet states T_2, T_3 may prove valuable.

The experimental observation of a prominent isomerization pathway adds to the discussion about the relative importance of atomic and molecular UV photoproduct yields of bromoform. Using vacuum ultraviolet resonance fluorescence spectroscopy, Bayes et al. determined a quantum yield of 0.76 ± 0.03 for the elimination of atomic Br radicals after 266 nm excitation (Channel I),[7] but left open the question of which products are responsible for the remaining 24% yield. Experiments by Xu et al. using time-of-flight mass spectrometry,[8] and by Huang et al. using cavity ring-down spectroscopy[16] determined molecular Br_2 product yields of 16%, 23%, and 26% for excitation with 267 nm, 248 nm, and 234 nm, respectively. Several other groups, however, have pointed out the possibility that a substantial fraction of Br_2 products may originate from multiphoton absorption processes during sequential, multistep excitation-dissociation processes.[9,14,15] Molecular elimination from polyhaloalkanes following multiphoton excitation has been well documented.[44-46] For single-photon excitation of bromoform with 248 nm, the upper limit for the Br_2 product yield has been estimated to 0.002 from VUV ionization photofragment translational spectroscopy,[9] and a transient XUV absorption study at 268 nm did not reveal any appreciable yield of Br_2 products within 10 ps after photoexcitation. Based on the signal-to-noise level of the experiment, the upper limit for Br_2 production within this timeframe was estimated to ~4%.[22] Calculated yields for UV-induced Br_2 elimination in isolated $CHBr_3$ are on the level of a few percent or less.[13,21] However, as the absolute rates for different relaxation pathways from the RRKM calculations deviate significantly from the ones observed in the UED experiment, there is a possibility that the branching ratio of atomic vs molecular products from isomer dissociation may also need to be reevaluated. The longer lifetime of the experimentally observed isomer compared to the theoretical estimate could provide the basis for a higher Br_2 product yield than originally predicted. An increased isomer lifetime extends the timescale available for intramolecular vibrational energy redistribution (IVR) and, thus, increases the chance that bonds other than the Br-Br bond be weakened and undergo scission. The observed indicators for a roaming type reaction mechanism involving >1.1 ps timescales may provide further opportunity for intramolecular radical-radical reactions that can lead to Br_2 abstraction.

Conclusion

The presented UED study firmly establishes isomerization as a very prominent relaxation pathway after 267 nm excitation of isolated bromoform molecules and provides key benchmarks regarding the isomer structure, dynamic preponderance, and a lower bound for the lifetime. The most obvious next steps to take are to extend the UED experiments to longer timescales and to further advance existing theoretical calculations. UED at extended pump-probe delays will determine the isoform lifetime and provide information on the relative yields of atomic versus molecular products emerging from isomer dissociation. Significantly expanded MD simulations[22] that include additional coupling mechanisms, cover longer trajectories with higher precision, and explore roaming as a potential pathway to iso-$CHBr_3$ would be extremely valuable to determine the fundamental mechanisms underlying the observed dynamics. We hope that the new experimental insights provided will stimulate such efforts.

AUTHOR INFORMATION

Corresponding Author

*Oliver Gessner – Chemical Sciences Division, Lawrence Berkeley National Laboratory, Berkeley, California 94720, USA; Email: ogessner@lbl.gov

Present Addresses

†Department of Chemistry, Tsinghua University, Beijing 100084, China.

§Diamond Light Source, Harwell Science & Innovation Campus, Didcot OX11 0DE, United Kingdom.

ξXi'an Institute of Optics and Precision Mechanics, Chinese Academy of Sciences, Xi'an, Shaanxi, 710119, China.

ηDepartment of Physics, University of Duisburg-Essen 47052 Duisburg, Germany; Department of Physics, University Dortmund, 44221 Dortmund, Germany; Research Center Chemical Sciences and Sustainability, Research Alliance Ruhr, 44780 Bochum, Germany.

Notes

The authors declare no competing financial interest.

Supporting Information

Experiment temporal resolution; pump photon absorption estimate; data acquisition and analysis; molecular structure fit in momentum space; comparison of UED results and MD simulations.

ACKNOWLEDGMENT

L.H., B.W.T., C.A.S., D.M.N., S.R.L., and O.G. were supported by the Atomic, Molecular, and Optical Sciences Program of the U.S. Department of Energy, Office of Science, Office of Basic Energy Sciences, Chemical Sciences, Geosciences, and Biosciences Division, through Contract No. DE-AC02-05CH11231. MeV-UED is operated as part of the Linac Coherent Light Source at the SLAC National Accelerator Laboratory, supported by the U.S. Department of Energy, Office of Science, Office of Basic Energy Sciences under Contract No. DE-AC02-76SF00515. A.Z. acknowledges support from the Miller Institute for Basic Research in Science. M.Z. acknowledges funding by the Department of Energy (DE-SC0024123). J.P. F. N, S. B. M., and M. C. were supported by the Atomic, Molecular, and Optical Sciences Program of the U.S. Department of Energy, Office of Science, Office of Basic Energy Sciences, Chemical Sciences, Geosciences, and Biosciences Division, through Contract No. DE- SC0014170.

REFERENCES

(1) Molina, M. J.; Rowland, F. S. Stratospheric Sink for Chlorofluoromethanes: Chlorine Atom-Catalysed Destruction of Ozone. *Nature* **1974**, 249 (5460), 810–812.

(2) Papanastasiou, D. K.; McKeen, S. A.; Burkholder, J. B. The Very Short-Lived Ozone Depleting Substance CHBr3 (Bromoform): Revised UV Absorption Spectrum, Atmospheric Lifetime and Ozone Depletion Potential. *Atmospheric Chem. Phys*. **2014**, 14 (6), 3017–3025

(3) *Scientific Assessment of Ozone Depletion: 2010*; Global Research and Monitoring Project; 50; WMO (World Meteorological Organization): Geneva, 2011. https://ozone.unep.org/sites/default/files/2019-05/00-SAP-2010-Assement-report.pdf (accessed 2023-06-22).

(4) Garcia, R. R.; Solomon, S. A New Numerical Model of the Middle Atmosphere: 2. Ozone and Related Species. *J. Geophys. Res.* **1994**, 99 (D6), 12937–12951.

(5) Shoute, L. C. T.; Neta, P. Bromine Atom Complexes with Bromoalkanes: Their Formation in the Pulse Radiolysis of Di-, Tri-, and Tetrabromomethane and Their Reactivity with Organic Reductants. *J. Phys. Chem*. **1990**, 94 (6), 2447–2453.

(6) Peterson, K. A.; Francisco, J. S. Should Bromoform Absorb at Wavelengths Longer than 300 nm? *J. Chem. Phys.* **2002**, 117 (13), 6103–6107.

(7) Bayes, K. D.; Friedl, R. R.; Sander, S. P.; Toohey, D. W. Measurements of Quantum Yields of Bromine Atoms in the Photolysis of Bromoform from 266 to 324 nm. *J. Geophys. Res.* **2003**, 108 (D3), 4095.

(8) Xu, D.; Francisco, J. S.; Huang, J.; Jackson, W. M. Ultraviolet Photodissociation of Bromoform at 234 and 267 nm by Means of Ion Velocity Imaging. *J. Chem. Phys*. **2002**, 117 (6), 2578–2585.

(9) Zou, P.; Shu, J.; Sears, T. J.; Hall, G. E.; North, S. W. Photodissociation of Bromoform at 248 nm: Single and Multiphoton Processes. *J. Phys. Chem. A* **2004**, 108 (9), 1482–1488.

(10) Carrier, S. L.; Preston, T. J.; Dutta, M.; Crowther, A. C.; Crim, F. F. Ultrafast Observation of Isomerization and Complexation in the Photolysis of Bromoform in Solution. *J. Phys. Chem. A* **2010**, 114 (3), 1548–1555.

(11) Mereshchenko, A. S.; Butaeva, E. V.; Borin, V. A.; Eyzips, A.; Tarnovsky, A. N. Roaming-Mediated Ultrafast Isomerization of Geminal Tri-Bromides in the Gas and Liquid Phases. *Nat. Chem.* **2015**, 7 (7), 562–568.

(12) King, K. D.; Golden, D. M.; Benson, S. W. Kinetics and Thermochemistry of the Gas-Phase Bromination of Bromoform. C-H Bond Dissociation Energy in Bromoform and the C-Br Dissociation Energy in Carbon Tetrabromide. *J. Phys. Chem*. **1971**, 75 (7), 987–989.

(13) Kalume, A.; George, L.; Reid, S. A. Isomerization as a Key Path to Molecular Products in the Gas-Phase Decomposition of Halons. *J. Phys. Chem. Lett.* **2010**, 1 (20), 3090–3095.

(14) Liu, W.; Chang, B. Transient Frequency Modulation Spectroscopy and 266 nm Photodissociation of Bromoform. *J. Chin. Chem. Soc.* **2001**, 48 (3), 613–617.

(15) Yang, S.-X.; Hou, G.-Y.; Dai, J.-H.; Chang, C.-H.; Chang, B.-C. Spectroscopic Investigation of the Multiphoton Photolysis Reactions of Bromomethanes ($CHBr_3$, $CHBr_2Cl$, $CHBrCl_2$, and CH_2Br_2) at Near-Ultraviolet Wavelengths. *J. Phys. Chem. A* **2010**, 114 (14), 4785–4790.

(16) Huang, H.-Y.; Chuang, W.-T.; Sharma, R. C.; Hsu, C.-Y.; Lin, K.-C.; Hu, C.-H. Molecular Elimination of Br_2 in 248 nm Photolysis of Bromoform Probed by Using Cavity Ring-down Absorption Spectroscopy. *J. Chem. Phys*. **2004**, 121 (11), 5253–5260.

(17) George, L.; Kalume, A.; Esselman, B. J.; Wagner, J.; McMahon, R. J.; Reid, S. A. Spectroscopic and Computational Studies of Matrix-Isolated iso-$CHBr_3$: Structure, Properties, and Photochemistry of Iso-Bromoform. *J. Chem. Phys.* **2011**, 135 (12), 124503.

(18) Petro, B. J.; Tweeten, E. D.; Quandt, R. W. Dispersed Fluorescence and Computational Study of the 2 × 193 nm Photodissociation of $CHBr_3$ and CBr_4. *J. Phys. Chem. A* **2004**, 108 (3), 384–391.

(19) Kong, Q.; Khakhulin, D.; Shkrob, I. A.; Lee, J. H.; Zhang, X.; Kim, J.; Kim, K. H.; Jo, J.; Kim, J.; Kang, J.; Pham, V.-T.; Jennings, G.; Kurtz, C.; Spence, R.; Chen, L. X.; Wulff, M.; Ihee, H. Solvent-Dependent Complex Reaction Pathways of Bromoform Revealed by Time-Resolved X-Ray Solution Scattering and X-Ray Transient Absorption Spectroscopy. *Struct. Dyn*. **2019**, 6 (6), 064902.

(20) Pal, S. K.; Mereshchenko, A. S.; Butaeva, E. V.; El-Khoury, P. Z.; Tarnovsky, A. N. Global Sampling of the Photochemical Reaction Paths of Bromoform by Ultrafast Deep-UV through near-IR Transient Absorption and Ab Initio Multiconfigurational Calculations. *J. Chem. Phys*. **2013**, 138 (12), 124501.

(21) Borin, V. A.; Matveev, S. M.; Budkina, D. S.; El-Khoury, P. Z.; Tarnovsky, A. N. Direct Photoisomerization of CH_2I_2 vs. $CHBr_3$ in the Gas Phase: A Joint 50 fs Experimental and Multireference Resonance-Theoretical Study. *Phys. Chem. Chem. Phys*. **2016**, 18 (41), 28883–28892.

(22) Toulson, B. W.; Borgwardt, M.; Wang, H.; Lackner, F.; Chatterley, A. S.; Pemmaraju, C. D.; Neumark, D. M.; Leone, S. R.; Prendergast, D.; Gessner, O. Probing Ultrafast C–Br Bond Fission in the UV Photochemistry of Bromoform with Core-to-Valence Transient Absorption Spectroscopy. *Struct. Dyn.* **2019**, 6 (5), 054304.

(23) Shen, X.; Nunes, J. P. F.; Yang, J.; Jobe, R. K.; Li, R. K.; Lin, M.-F.; Moore, B.; Niebuhr, M.; Weathersby, S. P.; Wolf, T. J. A.; Yoneda, C.; Guehr, M.; Centurion, M.; Wang, X. J. Femtosecond Gas-Phase Mega-Electron-Volt Ultrafast Electron Diffraction. *Struct. Dyn.* **2019**, 6 (5), 054305.

(24) Weathersby, S. P.; Brown, G.; Centurion, M.; Chase, T. F.; Coffee, R.; Corbett, J.; Eichner, J. P.; Frisch, J. C.; Fry, R.; Gühr, M.; Hartmann, N.; Hast, C.; Hettel, R.; Jobe, R. K.; Jongewaard, E. N.; Lewandowski, J. R.; Li, R. K.; Lindenberg, A. M.; Makasyuk, I.; May, J. E.; McCormick, D.; Nguyen, M. N.; Reid, A. H.; Shen, X.; Sokolowski, K.; Vecchione, T.; Vetter, S. L.; Wu, J.; Yang, J.; Dürr, H. A.; Wang, X. J. Mega-Electron-Volt Ultrafast Electron Diffraction at SLAC National Accelerator Laboratory. *Rev Sci Instrum* **2015**, 86, 073702.

(25) Yang, J.; Guehr, M.; Vecchione, T.; Robinson, M. S.; Li, R.; Hartmann, N.; Shen, X.; Coffee, R.; Corbett, J.; Fry, A.; Gaffney, K.; Gorkhover, T.; Hast, C.; Jobe, K.; Makasyuk, I.; Reid, A.; Robinson, J.; Vetter, S.; Wang, F.; Weathersby, S.; Yoneda, C.; Wang, X.; Centurion, M. Femtosecond Gas Phase Electron Diffraction with MeV Electrons. *Faraday Discuss*. **2016**, 194, 563–581.

(26) Shen, X.; Li, R.; Wang, X.; Weathersby, S.; Yang, J. Ultrafast Mega-Electron-Volt Gas-Phase Electron Diffraction at SLAC National Accelerator Laboratory. *Proc. 9th Int Part. Accel. Conf* **2018**, IPAC2018.

(27) Li, R. K.; Hoffmann, M. C.; Nanni, E. A.; Glenzer, S. H.; Kozina, M. E.; Lindenberg, A. M.; Ofori-Okai, B. K.; Reid, A. H.; Shen, X.; Weathersby, S. P.; Yang, J.; Zajac, M.; Wang, X. J. Terahertz-Based Subfemtosecond Metrology of Relativistic Electron Beams. *Phys. Rev. Accel. Beams* **2019**, 22 (1), 012803.

(28) Epp, S. W.; Hada, M.; Zhong, Y.; Kumagai, Y.; Motomura, K.; Mizote, S.; Ono, T.; Owada, S.; Axford, D.; Bakhtiarzadeh, S.; Fukuzawa, H.; Hayashi, Y.; Katayama, T.; Marx, A.; Müller-Werkmeister, H. M.; Owen, R. L.; Sherrell, D. A.; Tono, K.; Ueda, K.; Westermeier, F.; Miller, R. J. D. Time Zero Determination for FEL Pump-Probe Studies Based on Ultrafast Melting of Bismuth. *Struct. Dyn.* **2017**, 4 (5), 054308.

(29) Linstrom, P. NIST Chemistry WebBook, NIST Standard Reference Database 69, 1997.

(30) Cumpson, P. J.; Seah, M. P. Random Uncertainties in AES and XPS: I: Uncertainties in Peak Energies, Intensities and Areas Derived from Peak Synthesis. *Surf. Interface Anal.* **1992**, 18 (5), 345–360.

(31) Pandey, A.; Poirier, B. Plumbing Potentials for Molecules with Up To Tens of Atoms: How to Find Saddle Points and Fix Leaky Holes. *J. Phys. Chem. Lett.* **2020**, 11 (15), 6468–6474.

(32) Li, S. L.; Truhlar, D. G. Full-Dimensional Ground- and Excited-State Potential Energy Surfaces and State Couplings for Photodissociation of Thioanisole. *J. Chem. Phys.* **2017**, 146 (6), 064301.

(33) Peterson, A. A. Acceleration of Saddle-Point Searches with Machine Learning. *J. Chem. Phys.* **2016**, 145 (7), 074106.

(34) Suits, A. G. Roaming Reactions and Dynamics in the van Der Waals Region. *Annu. Rev. Phys. Chem*. **2020**, 71 (1), 77–100.

(35) Townsend, D.; Lahankar, S. A.; Lee, S. K.; Chambreau, S. D.; Suits, A. G.; Zhang, X.; Rheinecker, J.; Harding, L. B.; Bowman, J. M. The Roaming Atom: Straying from the Reaction Path in Formaldehyde Decomposition. *Science* **2004**, 306 (5699), 1158–1161.

(36) Grubb, M. P.; Warter, M. L.; Suits, A. G.; North, S. W. Evidence of Roaming Dynamics and Multiple Channels for Molecular Elimination in NO_3 Photolysis. *J. Phys. Chem. Lett*. **2010**, 1 (16), 2455–2458.

(37) Grubb, M. P.; Warter, M. L.; Xiao, H.; Maeda, S.; Morokuma, K.; North, S. W. No Straight Path: Roaming in Both Ground- and Excited-State Photolytic Channels of $NO_3 \rightarrow NO + O_2$. *Science* **2012**, 335 (6072), 1075–1078.

(38) Suits, A. G. Roaming Atoms and Radicals: A New Mechanism in Molecular Dissociation. *Acc. Chem. Res.* **2008**, 41 (7), 873–881.

(39) Bowman, J. M.; Suits, A. G. Roaming Reactions: The Third Way. *Physics Today* **2011**, 64 (11), 33–37.

(40) Klippenstein, S. J.; Georgievskii, Y.; Harding, L. B. Statistical Theory for the Kinetics and Dynamics of Roaming Reactions. *J. Phys. Chem. A* **2011**, 115 (50), 14370–14381.

(41) Bowman, J. M. Roaming. *Molecular Physics* **2014**, 112 (19), 2516–2528.

(42) Burke, M. P.; Casavecchia, P.; Cavallotti, C.; Clary, D. C.; Doner, A.; Green, W. H.; Grinberg Dana, A.; Guo, H.; Heathcote, D.; Hochlaf, M.; Klippenstein, S. J.; Kuwata, K. T.; Lawrence, J. E.; Lourderaj, U.; Mebel, A. M.; Milesevic, D.; Mullin, A. S.; Nguyen, T. L.; Olzmann, M.; Orr-Ewing, A. J.; Osborn, D. L.; Pazdera, T. M.; Robertson, P. A.; Robinson, M. S.; Rotavera, B.; Seakins, P. W.; Shannon, R. J.; Shiels, O. J.; Suits, A. G.; Trevitt, A. J.; Troe, J.; Vallance, C.; Welz, O.; Zhang, F.; Zádor, J. The Reaction Step: General Discussion. *Faraday Discuss*. **2022**, 238, 320–354.

(43) Endo, T.; Neville, S. P.; Wanie, V.; Beaulieu, S.; Qu, C.; Deschamps, J.; Lassonde, P.; Schmidt, B. E.; Fujise, H.; Fushitani, M.; Hishikawa, A.; Houston, P. L.; Bowman, J. M.; Schuurman, M. S.; Légaré, F.; Ibrahim, H. Capturing Roaming Molecular Fragments in Real Time. *Science* **2020**, 370 (6520), 1072–1077.

(44) Marvet, U.; Zhang, Q.; Brown, E. J.; Dantus, M. Femtosecond Dynamics of Photoinduced Molecular Detachment from Halogenated Alkanes. I. Transition State Dynamics and Product Channel Coherence. *J. Chem. Phys.* **1998**, 109 (11), 4415–4427.

(45) Marvet, U.; Brown, E. J.; Dantus, M. Femtosecond Concerted Elimination of Halogen Molecules from Halogenated Alkanes. *Phys. Chem. Chem. Phys.* **2000**, 2 (4), 885–891.

(46) Zhang, Q.; Marvet, U.; Dantus, M. Femtosecond Dynamics of Photoinduced Molecular Detachment from Halogenated Alkanes. II. Asynchronous Concerted Elimination of I_2 from CH_2I_2. *J. Chem. Phys.* **1998**, 109 (11), 4428–4442.

Table of Contents artwork